Available online at www.sciencedirect.com
SCIENCE DIRECT®
Electric Power Systems Research 75 (2012) 57–66
ELECTRIC POWER SYSTEMS RESEARCH
www.elsevier.com/locate/epsr

Modelling and simulation of induction motors with inter-turn faults for diagnostics

M. Arkan [a], D. Kostic-Perovic [b], P.J. Unsworth [c,*]

[a] *Inonu University, Engineering Faculty, Electrical–Electronics Department, Malatya, Turkey*
[b] *Dana Corporation, Automotive Motion Technology Ltd., Andover, UK*
[c] *University of Sussex, School of Engineering and IT, Brighton BN1 9QT, UK*

Received 20 April 2011; received in revised form 10 August 2011; accepted 18 August 2011
Available online 4 May 2012

Abstract

This paper presents two orthogonal axis models for simulation of three-phase induction motors having asymmetrical windings and inter-turn short circuits on the stator. The first model assumes that each stator phase winding has a different number of turns. To model shorted stator turns, the second model assumes phase *as* has two windings in series, representing the unaffected portion and the shorted portion. It uses the results of the first model to transfer phase *as* to *qd* so that shorted portion is transferred to the *q* axis. Simulations results from the models are in good agreement with other studies and are compared with experiment carried out on a specially wound motor with taps to allow different number of turns to be shorted. The models have been successfully used to study the transient and steady state behaviour of the induction motor with short-circuited turns, and to test stator fault diagnostic algorithms operating in real time.

Keywords: Induction motors; Turn faults; Modelling; Diagnostics; Orthaogonal axis

1. Introduction

Because of costly machinery repair, extended process down time, and health and safety problems, a trend in modern industry is to focus attention and resources on fault detection and predictive maintenance strategies for industrial plant [1,2]. It is known that approximately 36% of induction motor failures are caused by failure of the stator winding, and it is believed that these faults begin as undetected turn-to-turn faults in a coil, which progress to catastrophic phase-to-phase or phase-to-ground short circuit faults [1,2]. To achieve prior warning of failure so that an orderly shut-down may be made to avoid catastrophic failure, shorted turns within a stator winding coil must be detected or predicted [1–5].

Modelling of induction motors with shorted turns is the first step in the design of turn fault detection systems [3]. Simulation of transient and steady state behaviour of motors with these models enable correct evaluation of the measured data by diagnostics techniques. The asymmetrical induction machine has been a subject of considerable interest. Brown and Butler [6] have utilized symmetrical component theory to establish a general method of analysis for operation of polyphase induction motors having asymmetrical primary connection. Jha and Murthy [7] have utilized rotating field concepts to develop a generalized theory of induction machines having asymmetrical windings on both stator and rotor. Winding-function-based models presented in Refs. [8,9], and models presented in Refs. [10,11] need motor geometrical design parameters.

The generalized theory of electrical machines incorporating orthogonal or *qd0* axis theory is generally accepted as the preferred approach to almost all types of transient and steady state phenomena [12]. The analysis of machines is greatly facilitated by the standard transformation

* Corresponding author.
E-mail addresses: markan@inonu.edu.tr (M. Arkan), dragica.kostic-perovic@dana.com (D. Kostic-Perovic), p.j.unsworth@sussex.ac.uk (P.J. Unsworth).

0378-7796/$ – see front matter © 2012 Elsevier B.V. All rights reserved.
doi:10.1016/j.epsr.2011.08.015

to *qd0* axis. The same transformation process can be applied to machines in which there are phase unbalances [13]. Hence, it is useful to extend this approach to also incorporate problems encountered with asymmetrical induction motors.

The aim of this paper is to present a useful and straightforward method to simulate inter-turn short circuits for diagnostic purposes. The fault can be simulated by disconnecting one or more turns making up a stator phase winding [9,14]. Firstly an induction motor model with unequal numbers of stator turns has been developed. Then using this model, a second model has been developed to simulate stator inter-turn short circuits. Models are simulated in Matlab® Simulink® and simulation results are presented. Results obtained are confirmed with a conventional asymmetrical motor model in a three-phase, non-orthogonal base, and by experimental results obtained from a specially wound motor.

2. Induction motor model with different numbers of stator turns

The model for a symmetrical three-phase induction motor is well known [15–18]. To derive equations for asymmetrical stator winding and rotor, the following assumptions have been made:

- each stator phase of the motor has a different number of turns, but uniform spatial displacement is assumed;
- magnetic saturation is not present.

With the appropriate subscripts *as*, *bs*, *cs*, *ar*, *br*, and *cr*, the voltage equations of the magnetically coupled stator and rotor circuits can be written as follows:

$$\mathbf{v}^s_{abc} = \mathbf{r}^s_{abc}\mathbf{i}^s_{abc} + p\lambda^s_{abc}, \qquad 0 = \mathbf{r}^r_{abc}\mathbf{i}^r_{abc} + p\lambda^r_{abc} \tag{1}$$

where $p = d/dt$. Applying a stationary reference frame transformation to this equation yields the corresponding *qd0* equations and Eq. (1) becomes

$$\mathbf{v}^s_{qd0} = \mathbf{r}^s_{qd0}\mathbf{i}^s_{qd0} + p\lambda^s_{qd0},$$

$$0 = \mathbf{r}^r_{qd0}\mathbf{i}^r_{qd0} - \omega_r \begin{bmatrix} 0 & 1 & 0 \\ -1 & 0 & 0 \\ 0 & 0 & 0 \end{bmatrix} \lambda^r_{qd0} + p\lambda^r_{qd0} \tag{2}$$

where $\mathbf{r}^s_{qd0} = \begin{bmatrix} r^s_{11} & r^s_{12} & r^s_{13} \\ r^s_{21} & r^s_{22} & r^s_{23} \\ r^s_{31} & r^s_{32} & r^s_{33} \end{bmatrix}$ and matrix elements are given in Appendix A and assuming $r_{ar} = r_{br} = r_{cr} = r_r$, $\mathbf{r}^r_{qd0} = r_r\,\mathbf{I}_{3x3}$.

In matrix notation, the flux linkages of the stator and rotor windings may be written in terms of the winding inductances and the current as

$$\begin{bmatrix} \lambda^s_{abc} \\ \lambda^r_{abc} \end{bmatrix} = \begin{bmatrix} \mathbf{L}^{ss}_{abc} & \mathbf{L}^{sr}_{abc} \\ \mathbf{L}^{rs}_{abc} & \mathbf{L}^{rr}_{abc} \end{bmatrix} \begin{bmatrix} \mathbf{i}^s_{abc} \\ \mathbf{i}^r_{abc} \end{bmatrix} \tag{3}$$

where stator and rotor inductances are $\mathbf{L}^{ss}_{abc} = \begin{bmatrix} L_{asas} & L_{asbs} & L_{ascs} \\ L_{bsas} & L_{bsbs} & L_{bscs} \\ L_{csas} & L_{csbs} & L_{cscs} \end{bmatrix}$, and $\mathbf{L}^{rr}_{abc} = \begin{bmatrix} L_{arar} & L_{arbr} & L_{arcr} \\ L_{brar} & L_{brbr} & L_{brcr} \\ L_{crar} & L_{crbr} & L_{crcr} \end{bmatrix}$ Because of symmetry, stator mutual inductances have $L_{asbs} = L_{bsac}$, $L_{ascs} = L_{csas}$ and $L_{bscs} = L_{csbs}$. Similarly rotor self- and mutual inductances have $L_{arar} = L_{brbr} = L_{crcr}$, and $L_{arbr} = L_{arcr} = L_{brar} = L_{brcr} = L_{crar} = L_{crbr}$, respectively.

Those of the stator-to-rotor mutual inductances are dependent on the rotor angle (orientated with respect to stator), therefore

$$\mathbf{L}^{sr}_{abc} = \begin{bmatrix} L_{asar}\cos\theta_r & L_{asbr}\cos\left(\theta_r + \frac{2\pi}{3}\right) & L_{ascr}\cos\left(\theta_r - \frac{2\pi}{3}\right) \\ L_{bsar}\cos\left(\theta_r - \frac{2\pi}{3}\right) & L_{bsbr}\cos\theta_r & L_{bscr}\cos\left(\theta_r + \frac{2\pi}{3}\right) \\ L_{csar}\cos\left(\theta_r + \frac{2\pi}{3}\right) & L_{csbr}\cos\left(\theta_r - \frac{2\pi}{3}\right) & L_{cscr}\cos\theta_r \end{bmatrix} \tag{4}$$

and $\mathbf{L}^{rs}_{abc} = \mathbf{L}^{sr'}_{abc}$ where $(')$ means the transpose of the matrix. The coefficients L_{asar}, L_{asbr}, L_{ascr}, L_{bsar}, L_{bsbr}, L_{bscr}, L_{csar}, L_{csbr}, and L_{cscr} are peak values of stator-to-rotor mutual inductances. Because of rotor symmetry $L_{asar} = L_{asbr} = L_{ascr}$, $L_{bsar} = L_{bsbr} = L_{cscr}$, and $L_{csar} = L_{csbr} = L_{cscr}$.

The stator and rotor *qd0* flux linkages are obtained by applying transformation to the stator and rotor *abc* flux linkages in Eq. (3), that is

$$\lambda^s_{qd0} = \mathbf{L}^{ss}_{qd0}\mathbf{i}^s_{qd0} + \mathbf{L}^{sr}_{qd0}\mathbf{i}^r_{qd0},$$

$$\lambda^r_{qd0} = \mathbf{L}^{rs}_{qd0}\mathbf{i}^s_{qd0} + \mathbf{L}^{rr}_{qd0}\mathbf{i}^r_{qd0} \tag{5}$$

where $\mathbf{L}^{ss}_{qd0} = \begin{bmatrix} L^{ss}_{11} & L^{ss}_{12} & L^{ss}_{13} \\ L^{ss}_{21} & L^{ss}_{22} & L^{ss}_{23} \\ L^{ss}_{31} & L^{ss}_{32} & L^{ss}_{33} \end{bmatrix}$, $\mathbf{L}^{sr}_{qd0} = \begin{bmatrix} L^{sr}_{11} & L^{sr}_{12} & 0 \\ L^{sr}_{21} & L^{sr}_{22} & 0 \\ L^{sr}_{31} & L^{sr}_{32} & 0 \end{bmatrix}$, $\mathbf{L}^{rr}_{qd0} = \begin{bmatrix} L^{rr}_{11} & 0 & 0 \\ 0 & L^{rr}_{22} & 0 \\ 0 & 0 & L^{rr}_{33} \end{bmatrix}$, and

$\mathbf{L}^{rs}_{qd0} = \begin{bmatrix} L^{sr}_{11} & L^{sr}_{21} & 0.5\,L^{sr}_{31} \\ L^{sr}_{12} & L^{sr}_{22} & -0.5\,L^{sr}_{32} \\ 0 & 0 & 0 \end{bmatrix}$. Matrix elements of $\mathbf{L}^{ss}_{qd0}$, $\mathbf{L}^{sr}_{qd0}$, $\mathbf{L}^{rr}_{qd0}$, and $\mathbf{L}^{rs}_{qd0}$ are given in Appendix A.

Normally, an induction machine is connected to a three-phase supply by a three-wire connection (i.e. neutral current does not flow). Hence, for a squirrel cage induction machine and three-wire connection, the stator and rotor flux linkages in Eq. (5) may be expressed compactly as

$$\begin{bmatrix} \lambda^s_q \\ \lambda^s_d \\ \lambda^r_q \\ \lambda^r_d \end{bmatrix} = \begin{bmatrix} L^{ss}_{11} & L^{ss}_{12} & L^{sr}_{11} & L^{sr}_{12} \\ L^{ss}_{21} & L^{ss}_{22} & L^{sr}_{21} & L^{sr}_{22} \\ L^{sr}_{11} & L^{sr}_{12} & L^{rr}_{11} & 0 \\ L^{sr}_{21} & L^{sr}_{22} & 0 & L^{rr}_{22} \end{bmatrix} \begin{bmatrix} i^s_q \\ i^s_d \\ i^r_q \\ i^r_d \end{bmatrix} \tag{6}$$

2.1. Determination of inductances

In order to define asymmetrical machine inductances, assume stator phases *as*, *bs* and *cs* have numbers of winding turns given by N_a, N_b, and N_c, respectively, and that rotor phases *ar*, *br* and *cr* have winding turns given by $N_{ar}=N_{br}=N_{cr}=N_r$. If self- and mutual inductances are known for a symmetrical machine with reference number of turns N_s, new parameters for an asymmetrical machine can be defined from these inductance values as described in [2,15,18].

By using known parameters the stator self-inductances for phases *as*, *bs* and *cs* can be calculated as

$$L_{asas} = \frac{N_a^2}{N_s^2}\left(L_{ls} + \frac{2}{3}L_m\right) = N_a^2 L_{mls} \tag{7}$$

$$L_{bsbs} = N_b^2 L_{mls} \tag{8}$$

$$L_{cscs} = N_c^2 L_{mls} \tag{9}$$

where $L_{mls} = \frac{1}{N_s^2}\left(L_{ls} + \frac{2}{3}L_m\right)$.

The stator mutual inductances between phases *as* and *bs*, *bs* and *cs*, and *cs* and *as* can be derived as

$$L_{asbs} = L_{bsas} = \left(-\frac{1}{2}N_aN_b\right)\left(\frac{2}{3}\frac{L_m}{N_s{}^2}\right) = -\frac{1}{3}\frac{N_aN_b}{N_s^2}L_m = N_aN_bL_{mss} \tag{10}$$

$$L_{ascs} = L_{csas} = N_aN_cL_{mss} \tag{11}$$

$$L_{bscs} = L_{csbs} = N_bN_cL_{mss} \tag{12}$$

where $L_{mss} = -\frac{1}{3}\frac{L_m}{N_s^2}$.

The rotor self- and mutual inductances can be found by a similar way. Because the rotor is assumed symmetric, the total self-inductances of rotor phases *ar*, *br* and *cr* are equal. Therefore

$$L_{arar} = L_{brbr} = L_{crcr} = L_{lr} + \frac{2}{3}\frac{N_r^2}{N_s^2}L_m = L_{lr} + L_{mar} \tag{13}$$

where $L_{mar} = \frac{2}{3}\frac{N_r^2}{N_s^2}L_m$. For the same reason, rotor mutual inductances are also equal to each other and given by

$$L_{arbr} = L_{arcr} = L_{brar} = L_{brcr} = L_{crar} = L_{crbr} = -\left(\frac{1}{2}\right)\left(\frac{2}{3}\frac{N_r^2}{N_s^2}L_m\right) = -\frac{1}{2}L_{mar} \tag{14}$$

Previously defined stator-to-rotor mutual inductances can be defined in term of new parameters. Because of rotor symmetry (turn numbers for each rotor phase are equal) mutual inductances will be $L_{asar}=L_{asbr}=L_{ascr}$, $L_{bsar}=L_{bsbr}=L_{bscr}$, and $L_{csar}=L_{csbr}=L_{cscr}$.

Referring to Fig. 1, we can see that the rotor phase *ar* is displaced from stator phase *as* by the electrical angle θ_r, where θ_r is a variable. The corresponding mutual inductances will vary with θ_r. The variable sine and cosine factors are already present in Eq. (4), so peak mutual inductances will be

$$L_{asar} = L_{asbr} = L_{ascr} = \frac{2}{3}\frac{N_aN_r}{N_s^2}L_m = N_aL_{msr} \tag{15}$$

$$L_{bsar} = L_{bsbr} = L_{bscr} = \frac{2}{3}\frac{N_bN_r}{N_s^2}L_m = N_bL_{msr} \tag{16}$$

$$L_{csar} = L_{csbr} = L_{cscr} = \frac{2}{3}\frac{N_cN_r}{N_s^2}L_m = N_cL_{msr} \tag{17}$$

where $L_{msr} = \frac{2}{3}\frac{N_r}{N_s^2}L_m$.

2.2. Simulation of the asymmetrical induction motors

In this subsection, equations are rearranged for the asymmetrical induction motor model that has been developed.

The *qd*-applied voltage in a reference frame fixed to the stator can be obtained from the stator phase voltage v_{as}, v_{bs}, and v_{cs} by standard transformation [17]. The *qd* voltages will be

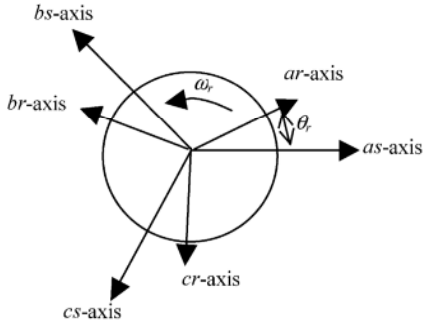

Fig. 1. Induction machine winding displacement.

$$v_q^s = \frac{2}{3}\left[v_{as} - \frac{1}{2}(v_{bs} + v_{cs})\right] = \frac{2}{3}\left[v_{ag} - \frac{1}{2}(v_{bg} + v_{cg})\right],$$

$$v_d^s = \frac{1}{\sqrt{3}}(-v_{bs} + v_{cs}) = \frac{1}{\sqrt{3}}(-v_{bg} + v_{cg}) \quad (18)$$

where v_{ag}, v_{bg}, and v_{cg} are supply phase voltages.

Flux linkages may be obtained from Eq. (2) for a three-wire system to give

$$\lambda_q^s = \int (v_q^s - r_{11}^s i_q^s - r_{12}^s i_d^s)\,\mathrm{d}t,$$

$$\lambda_d^s = \int (v_d^s - r_{21}^s i_q^s - r_{22}^s i_d^s)\,\mathrm{d}t,$$

$$\lambda_q^r = \int (\omega_r \lambda_d^r - r_r^r i_q^r)\,\mathrm{d}t,$$

$$\lambda_d^r = -\int (\omega_r \lambda_q^r + r_r^r i_d^r)\,\mathrm{d}t \quad (19)$$

The current can be found by inverting Eq. (6).

The speed of the machine can be obtained from the torque equation as

$$\omega_r(t) = \frac{P}{2J}\int (T_{\mathrm{em}} + T_{\mathrm{mech}} - T_{\mathrm{damp}})\,\mathrm{d}t \quad (20)$$

T_{em} is the electromagnetic torque impressed on the shaft of the machine and can be expressed as

$$T_{\mathrm{em}} = \frac{3}{2}\frac{P}{2}(\lambda_d^s i_q^s - \lambda_q^s i_d^s) \quad (21)$$

T_{mech} is the externally applied mechanical torque in the direction of the rotor speed, T_{damp} is the damping torque in the opposite direction of the rotor speed, and J is inertia.

By using Eqs. (18)–(21) with resistances and inductances that are defined in Appendix A, a motor with asymmetrical windings can be simulated. The compact model for the simulation of the asymmetrical motor is shown in Fig. 2.

Results of simulation in Fig. 2 are fed to a diagnostic block that uses negative sequence current to display motor condition. Supply voltage and motor current are decomposed into their positive and negative sequence components by using a power decomposition technique [19] and the condition of the motor is analysed using a method that has been described in [2,4,20].

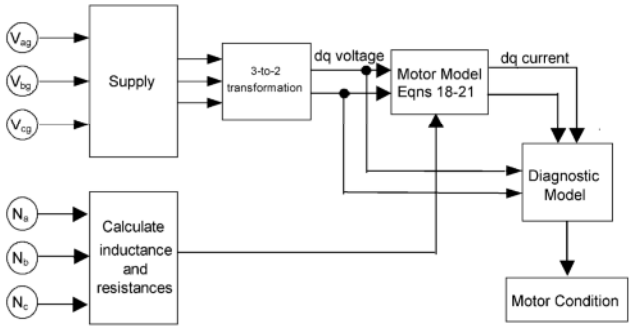

Fig. 2. Simulation of asymmetrical induction motor model.

3. Induction motor model with inter-turn stator short circuit

In order to develop an induction motor model with a stator inter-turn short circuit, it has been assumed that phase *as* has two windings in series comprising N_{us} unshorted turns and N_{sh} shorted turn(s), where $N_{as} = N_{us} + N_{sh} = N_s$, the overall number of turns N_s. The phases *bs* and *cs* have $N_{bs} = N_{cs} = N_s$. By assuming the unequal numbers of stator turns, the first model can be used for induction motor model with inter-turn short circuit to transfer motor equation from *abc* axes to *qd0* axes. By doing this, the N_{sh} turn shorted winding can be introduced in *qd0* axes. The fault severity can be changed by varying the number of shorted turns, and by a current limiting resistance across the short circuit windings. The same assumptions that were made for the first model are valid for this model as well.

In the following, the modification of equations for the new model is presented.

The self-inductances for phase *as, bs,* and *cs* in Eqs. (7)–(9) will be

$$\begin{aligned} L_{asas} &= \frac{N_{us}^2}{N_s^2}\left(L_{ls} + \frac{2}{3}L_m\right) + 2N_{us}N_{sh}\left(\frac{2}{3}\frac{L_m}{N_s^2}\right) \\ &\quad + \frac{N_{sh}^2}{N_s^2}\left(L_{ls} + \frac{2}{3}L_m\right) \\ &= (N_{us}^2 L_{mls} + N_{us}N_{sh}L_{msh}) \\ &\quad + (N_{us}N_{sh}L_{msh} + N_{sh}^2 L_{mls}) \\ &= (L'_{asas} + L_{assh}) + (L_{assh} + L_{shsh}) \end{aligned} \quad (22)$$

where $L_{msh} = \frac{2}{3}\frac{L_m}{N_s^2}$ and subscript '*sh*' is used for shorted winding(s).

$$L_{bsbs} = L_{cscs} = \frac{N_s^2}{N_s^2}\left(L_{ls} + \frac{2}{3}L_m\right) = N_s^2 L_{mls} \quad (23)$$

As it can be seen from Eq. (22), the phase *as* self-inductance contains the unshorted self-inductance L'_{asas}, the mutual inductance between unshorted and shorted turns L_{assh}, and the shorted turns self-inductance L_{shsh}.

The stator mutual inductances will be

$$\begin{aligned} L_{asbs} &= -\frac{1}{3}\frac{N_a N_s}{N_s^2}L_m = -\frac{1}{3}\frac{N_{us}}{N_s}L_m - \frac{1}{3}\frac{N_{sh}}{N_s}L_m \\ &= L'_{asbs} + L_{shbs} \end{aligned} \quad (24)$$

$$L_{ascs} = L_{bsas} = L_{csas} = L'_{asbs} + L_{shbs},$$

$$L_{bscs} = L_{csbs} = -\frac{1}{3}L_m \quad (25)$$

The stator-to-rotor mutual inductances in Eqs. (15)–(17) will be

$$L_{asr} = L_{asar} = L_{asbr} = L_{ascr} = \frac{2}{3}\frac{N_a N_r}{N_s^2} L_m$$
$$= \frac{2}{3}\frac{N_{us} N_r}{N_s^2} L_m + \frac{2}{3}\frac{N_{sh} N_r}{N_s^2} L_m = L'_{asar} + L_{shar} \quad (26)$$

$$L_{bsr} = L_{bsar} = L_{bsbr} = L_{bscr} = L_{csar} = L_{csbr} = L_{cscr}$$
$$= \frac{2}{3}\frac{N_s N_r}{N_s^2} L_m \quad (27)$$

As in the previous section, assuming that stator windings have different numbers of turns, *dq0* axes inductances can be obtained for an inter-turn short circuit condition by using the newly defined self- and mutual inductances. The transformations of $\mathbf{L}^{ss}_{abc}$ to $\mathbf{L}^{ss}_{qd0}$ and $\mathbf{L}^{sr}_{abc}$ to $\mathbf{L}^{sr}_{qd0}$ are

$$\mathbf{L}^{ss}_{qd0} = \begin{bmatrix} L^{ss}_{11} & 0 & L^{ss}_{13} \\ 0 & L^{ss}_{22} & 0 \\ L^{ss}_{31} & 0 & L^{ss}_{33} \end{bmatrix} \text{ and}$$
$$\mathbf{L}^{sr}_{qd0} = \begin{bmatrix} L^{sr}_{11} & 0 & 0 \\ 0 & L^{sr}_{22} & 0 \\ L^{sr}_{31} & 0 & 0 \end{bmatrix} \quad (28)$$

where $L^{ss}_{11} = (L^{s}_{q} + L^{ssh}_{q}) + (L^{sh}_{q} + L^{ssh}_{q})$, $L^{ss}_{22} = L^{s}_{d}$, $L^{sr}_{11} = L^{sr}_{q} + L^{shr}_{q}$ and $L^{sr}_{22} = L^{sr}_{d}$.

Similarly, the results of transformation of rotor self- and mutual inductances can be simplified as

$$\mathbf{L}^{rr}_{qd0} = \begin{bmatrix} L^{rr}_{11} & 0 & 0 \\ 0 & L^{rr}_{22} & 0 \\ 0 & 0 & L^{rr}_{33} \end{bmatrix} \text{ and}$$
$$\mathbf{L}^{rs}_{qd0} = \begin{bmatrix} L^{sr}_{11} & 0 & 0.5L^{sr}_{31} \\ 0 & L^{sr}_{22} & 0 \\ 0 & 0 & 0 \end{bmatrix} \quad (29)$$

where $L^{rr}_{11} = L^{r}_{q}$ and $L^{rr}_{22} = L^{r}_{d}$. Matrix elements are given in Appendix A.

The stator and rotor flux linkages for the new model of a squirrel cage induction motors will be

$$\begin{bmatrix} \lambda^{sh}_q \\ \lambda^{s}_q \\ \lambda^{s}_d \\ \lambda^{r}_q \\ \lambda^{r}_d \end{bmatrix} = \begin{bmatrix} L^{sh}_q & L^{ssh}_q & 0 & L^{shr}_q & 0 \\ L^{ssh}_q & L^{s}_q & 0 & L^{sr}_q & 0 \\ 0 & 0 & L^{s}_d & 0 & L^{sr}_d \\ L^{shr}_q & L^{sr}_q & 0 & L^{r}_q & 0 \\ 0 & 0 & L^{sr}_d & 0 & L^{r}_d \end{bmatrix} \begin{bmatrix} i^{sh}_q \\ i^{s}_q \\ i^{s}_d \\ i^{r}_q \\ i^{r}_d \end{bmatrix} \quad (30)$$

The stator phase resistances are

$$r_{as} = \frac{N_a}{N_s} r_s = \frac{N_{us}}{N_s} r_s + \frac{N_{sh}}{N_s} r_s = r'_{as} + r_{sh} \quad (31)$$

$$r_{bs} = r_{cs} = r_s \quad (32)$$

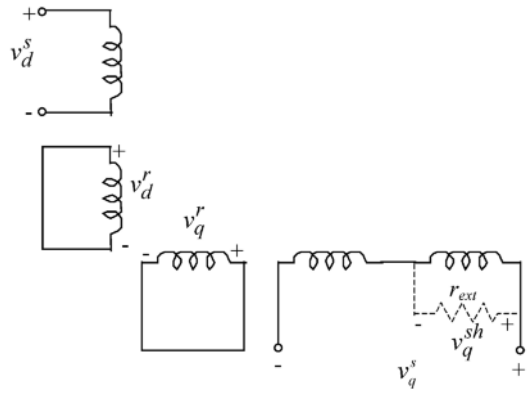

Fig. 3. Motor model with inter-turn stator short circuit.

where r_{sh} is the shorted winding(s) resistance. Stator *qd* resistance for new model will be

$$\begin{bmatrix} r^{sh}_q \\ r^{s}_q \\ r^{s}_d \end{bmatrix} = \begin{bmatrix} \frac{2}{3} r_{sh} & 0 & 0 \\ 0 & r^{s}_{11} & r^{s}_{12} \\ 0 & r^{s}_{21} & r^{s}_{22} \end{bmatrix} \quad (33)$$

The shorted portion of the stator winding (*sh*) is seen to only appear in the *q*-axis element. The matrix elements are given in Appendix A. Fig. 3 shows the motor model with an inter-turn short circuit, which only effects part of the *q*-axis stator winding. r_{ext} is an external short circuit current limiting resistance.

Flux linkages may be obtained from Eq. (2) for a three-wire system in the stationary reference frame to give

$$\lambda^{sh}_q = \int (v^{sh}_q - r_{sh} i^{sh}_q)\,\mathrm{d}t,$$
$$\lambda^{s}_q = \int (v^{s}_q - v^{sh}_q - r^{s}_{11} i^{s}_q - r^{s}_{12} i^{s}_d)\,\mathrm{d}t,$$
$$\lambda^{s}_d = \int (v^{s}_d - r^{s}_{21} i^{s}_q - r^{s}_{22} i^{s}_d)\,\mathrm{d}t,$$
$$\lambda^{r}_q = \int (\omega_r \lambda^{r}_d - r^{r}_r i^{r}_q)\,\mathrm{d}t,$$
$$\lambda^{r}_d = -\int (\omega_r \lambda^{r}_q + r^{r}_r i^{r}_d)\,\mathrm{d}t \quad (34)$$

Note that v^{sh}_q will be zero if the external resistance r_{ext} is zero. The current can be found by inverting Eq. (30).

4. Simulation results

The models developed have been simulated in Matlab® Simulink® and the following simulation results are for a 2 hp motor whose parameters are given in Appendix A. The results are taken during acceleration from stand still to full speed.

Figs. 4 and 5 are results for acceleration from stand still to full speed at full load under normal conditions. Initially, motor currents are not symmetrical because of the starting

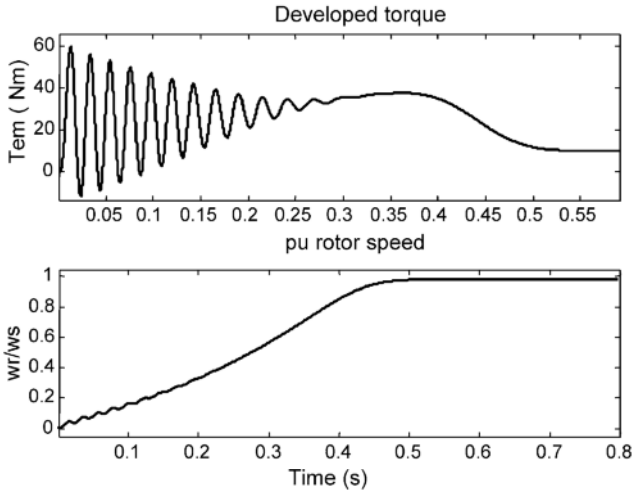

Fig. 4. Torque and speed variation.

transient. This introduces high negative sequence current until the motor reaches full speed.

Figs. 6 and 7 show the simulation results from stand still to full speed at full load with five turns shorted. The supply negative sequence current is around 400 mA. Because of stator asymmetry, the torque graph in Fig. 6 shows the expected pulsation at twice supply frequency ($2f_s$) even at steady state. This is because the negative sequence current introduces a braking torque in the motor. The short circuit current of 60 A in the shorted turns seen in Fig. 7 is 2.6 times the normal locked rotor current of 23 A.

Figs. 8 and 9 are for same condition but with an external 1.5 Ω resistance to limit short circuit current to avoid destruction of the motor. This limits short circuit current to nearly 3 A, and supply negative sequence current to 27 mA. The torque still has pulsation $2f_s$ but is much smaller as seen in Fig. 8.

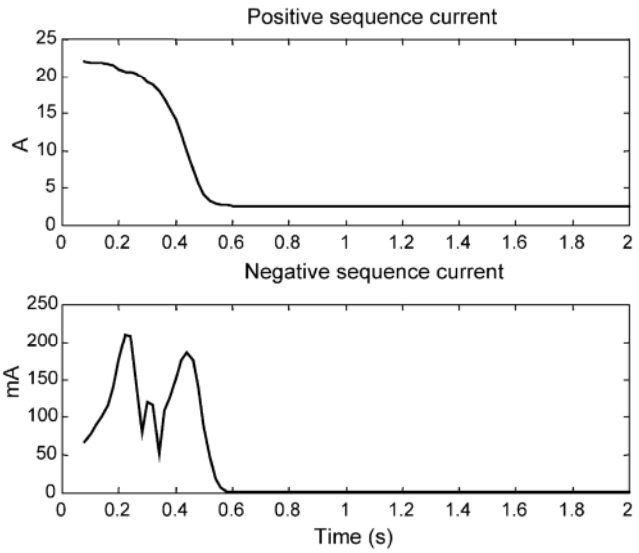

Fig. 5. Positive and negative sequence currents (rms).

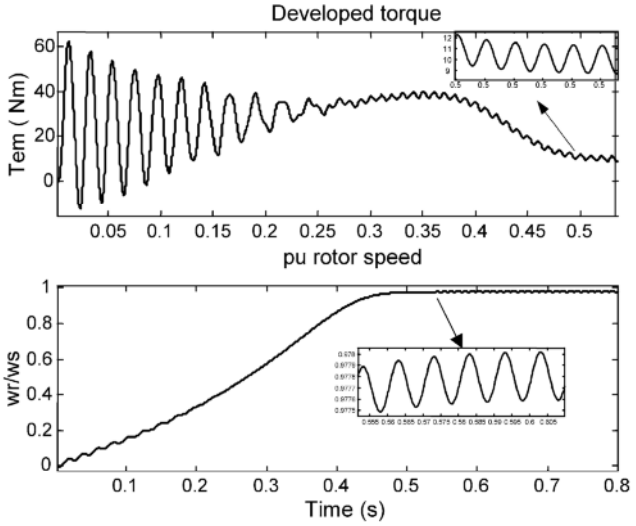

Fig. 6. Torque and speed variation with five turns shorted.

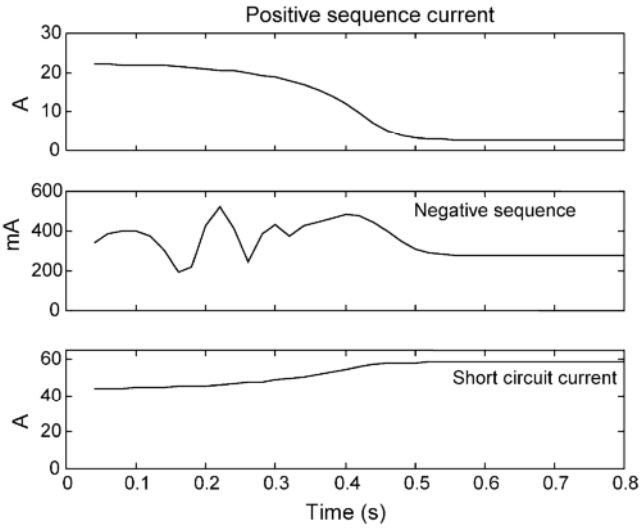

Fig. 7. Positive sequence, negative sequence, and short circuit currents for five turns shorted.

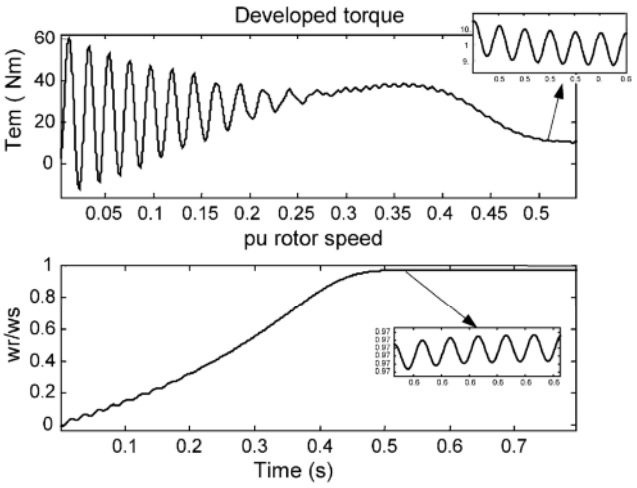

Fig. 8. Torque and speed variation with five turns shorted with 1.5 Ω resistance.

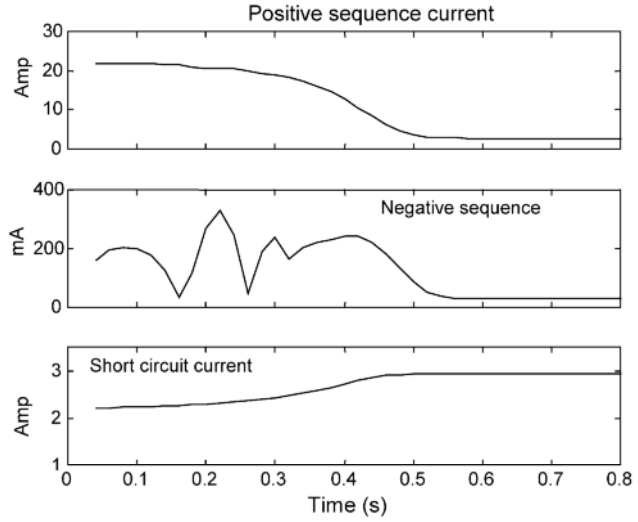

Fig. 9. Positive sequence, negative sequence and short circuit currents for five turns shorted with 1.5 Ω resistance.

4.1. Comparison of experimental with simulated results

In order to validate the results from the dynamic model developed, an experimental investigation was also conducted. The results in Table 1 compare experimental results with simulation results obtained for a specially wound 2 hp motor with up to four turns shorted. Experimental and simulated short circuit currents have been limited by using an external 0.3 Ω r_ext resistance. I_n is motor negative sequence current, and I_{r_ext} is short circuit current in the external current limiting resistance.

4.2. Relation between shorted turns and negative sequence current

Results have also been obtained by simulation for different numbers of directly shorted turns ($r_{ext} = 0$). For $r_{ext} = 0$ negative sequence current I_n is proportional to the number n of shorted turns

$$I_n \propto n \quad \text{or} \quad I_n \cong kn \tag{35}$$

where k is constant.

Fig. 10 shows I_{r_ext} current in the external resistance and number of shorted turns relation with 0 and 0.2 Ω external current limiting resistance. As it can be seen from figure short

Table 1
Experimental and simulation results for different numbers of shorted turns with short circuit current limited externally

n	Experimental result		Simulation result	
	I_n (mA)	I_{r_ext} (A)	I_n (mA)	I_{r_ext} (A)
1	4	2.7	5.6	2.9
2	15	5.3	16	5.6
3	30	8.98	31.4	8.1
4	54	10	48.5	10.2

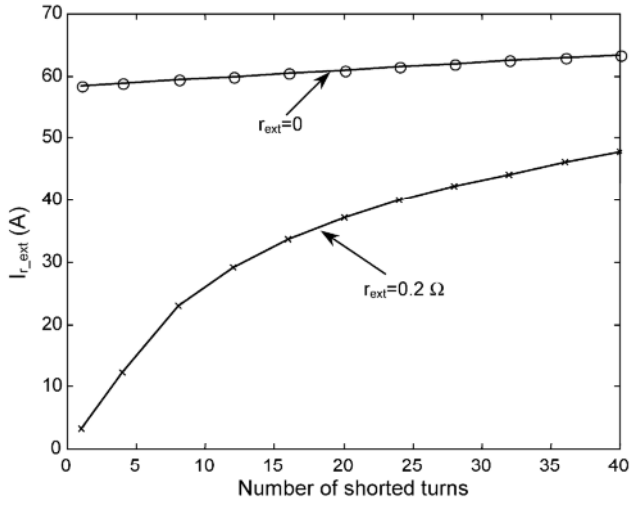

Fig. 10. Short circuit current vs. shorted turns for different external resistance values (r_{ext}).

circuit current is almost independent of the number of shorted turn when external resistance is zero, at 2.6 times locked rotor current. This means that for a short circuit fault involving only few turns, the motor will run for a considerable time, from a few minutes to an hour, since the shorted turns can dissipate heat into adjacent turns. In addition, as their temperature rises, their resistance increases, and Fig. 10 shows that the current reduces quite rapidly with additional resistance within the short circuit path (r_{ext} in the experimental study).

Fig. 11 presents relation between the number of shorted turns, external current limiting resistance, and negative sequence current.

4.3. Effect of unequal winding temperatures

If a motor is operated from an unbalanced voltage supply, the heating effect of unequal phase currents will cause

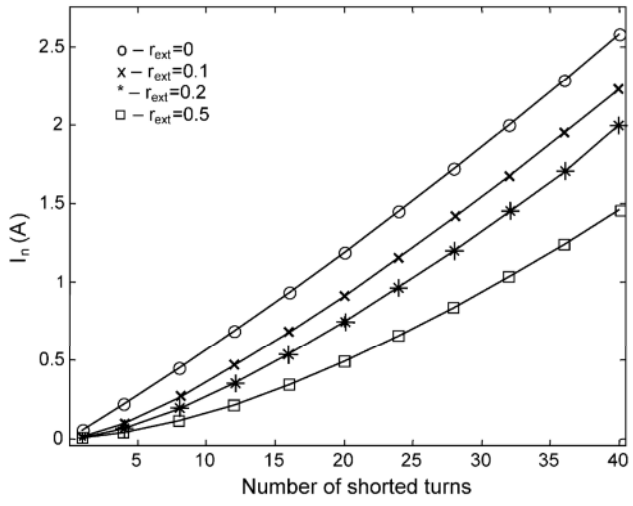

Fig. 11. Negative sequence current vs. shorted turns for different external resistance values (r_{ext}). Short circuit current limited by 0, 0.1, 0.2 and 0.5 Ω resistance.

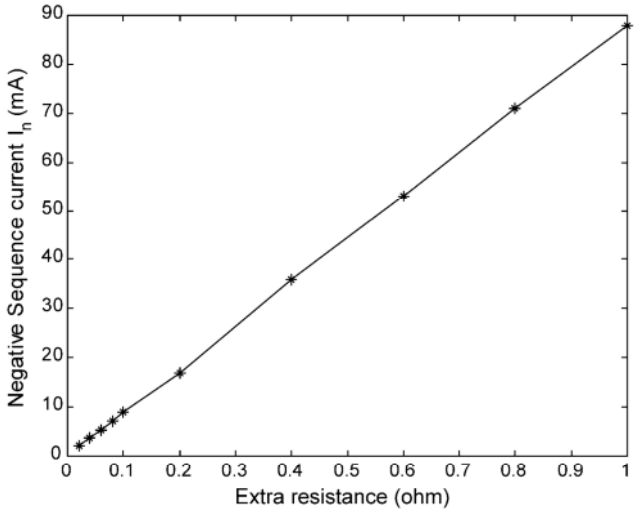

Fig. 12. Negative sequence current vs. extra series resistance r_{unb}.

resistive unbalance to develop between the phases, whose contribution to negative sequence current could be confused with a stator fault. This is now considered.

Assuming an additional temperature rise in only one motor phase, its effect may be obtained by considering an unbalance resistance r_{unb} in series with stator phase *as*. The maximum added resistance r_{unb} is 1 Ω which is equivalent to a 61.5 °C temperature rise. I_n is linearly proportional to r_{unb} (see Fig. 12).

$$I_n \propto r_{unb} \tag{36}$$

The relation between r_{unb} and negative sequence current can be defined [2] as

$$I_n = \frac{r_{unb}}{3} \frac{I_{sp}}{Z_n + (r_{unb}/3)} \tag{37}$$

where I_{sp} is positive sequence current, $Z_n = \left| r_s + \frac{r_r}{2-s_p} + j(X_s + X_r) \right|$, and if $Z_n \gg \frac{r_{unb}}{3}$ the above equation can be simplified to

$$I_n = \frac{r_{unb}}{3} \frac{I_{sp}}{Z_n} \tag{38}$$

under balanced supply conditions.

The relation between negative sequence and the number of shorted turns n is presented in [2] as

$$I_n = \frac{3}{8} \frac{n}{N_s} \frac{V_{sp}}{Z_s} \tag{39}$$

where V_{sp} is the applied positive sequence voltage, N_s the total number of turns, n the number of shorted turn, and $Z_s = |r_s + jX_s|$. The relation between r_{unb} and n to give the same negative sequence current can be defined from Eqs. (38) and (39)

$$\frac{r_{unb}}{n} = \frac{9}{8} \frac{1}{N} \frac{Z_n}{Z_s} \frac{V_{sp}}{I_{sp}} \tag{40}$$

With the motor parameters used in the simulations (see Appendix A) at rated voltage 240 V and full-load current 2.7 A, Eq. (40) can be simplified to

$$r_{unb} = 0.69n\ \Omega \tag{41}$$

From simulation results, $r_{unb} = 0.63n\ \Omega$ is obtained, which is close to the theoretical relation (Eq. (41)).

Hence a thermal increase in resistance of one phase (due to current unbalance) by 0.69 Ω relative to the other windings will give the same effect as a single turn short circuit. For the motor used, this is a 17% increase, which is equivalent to a 42.5 °C increase in temperature in one winding over the other windings.

5. Conclusion

Two models have been developed for analysing an asymmetrical induction motor. The models are based on general machine parameters so that it is not necessary to know detailed motor geometry or physical layout of the windings. New parameters for asymmetrical conditions have been presented. The models have also been confirmed against simulation results obtained from a conventional asymmetrical motor model in a three phase non-orthogonal base, which requires seven differential equations. It has not been presented because of space.

Inter-turn faults can be easily simulated by the model. Fault severity can be controlled by the number of shorted turns and an optional current limiting resistance to short circuit the windings. Simulation results have been used in [2,4,20,21] to check fault detection algorithms for stator faults.

The models have been used to study the relation between the number of shorted turns and negative sequence current, the effects of resistive unbalance between the phases due to the heating effect of unbalanced phase currents, and temperature effects on shorted turn resistance. Results confirm that negative sequence current and shorted number of turns are linearly dependant, and that resistive unbalance can produce comparable negative sequence current, so that fault detection algorithms should be able to distinguish between the effects of turn shorts and thermal unbalance [2,4,20]. The results obtained for short circuit under limited short circuit current (by external resistance) reveal that sensitivity depends on number of shorted turns and short circuit current.

Acknowledgements

The authors thank Dr. Peter Lindon for providing a conventional asymmetrical motor model in a three-phase non-orthogonal base to validate the developed models, and for his valuable discussions.

Appendix A

A.1. Matrix elements for induction motor with different numbers of stator turns

The *qd0* resistances elements are:

$$r_{11}^{s} = \frac{2}{3}\left(r_{as} + \frac{1}{4}r_{bs} + \frac{1}{4}r_{cs}\right) \tag{42}$$

$$r_{12}^{s} = \frac{\sqrt{3}}{6}(r_{bs} - r_{cs}) \tag{43}$$

$$r_{13}^{s} = \frac{1}{3}(2r_{as} - r_{bs} - r_{cs}) \tag{44}$$

$$r_{22}^{s} = \frac{1}{2}(r_{bs} + r_{cs}) \tag{45}$$

$$r_{33}^{s} = \frac{1}{3}(r_{as} + r_{bs} + r_{cs}) \tag{46}$$

$r_{21}^{s} = r_{12}^{s}$, $r_{23}^{s} = -\frac{1}{2}r_{12}^{s}$, $r_{31}^{s} = \frac{1}{2}r_{13}^{s}$, and $r_{32}^{s} = -r_{12}^{s}$, where $r_{as} = \frac{N_a}{N_s}r_s$, $r_{bs} = \frac{N_b}{N_s}r_s$, and $r_{cs} = \frac{N_c}{N_s}r_s$, when $N_a = N_b = N_c = N_s$, $r_{11}^{s} = r_{22}^{s} = r_{33}^{s} = r_s$ and $r_{12}^{s} = r_{13}^{s} = r_{21}^{s} = r_{23}^{s} = r_{31}^{s} = r_{32}^{s} = 0$.

A.2. The stator qd0 self- and mutual inductances

$\mathbf{L}_{qd0}^{ss}$ matrix elements are:

$$L_{11}^{ss} = \frac{2}{3}(L_{asas} + .25L_{bsbs} + .25L_{cscs} - L_{asbs} - L_{ascs} + .5L_{bscs}) \tag{47}$$

$$L_{12}^{ss} = \frac{1}{2\sqrt{3}}(L_{bsbs} - L_{cscs} - L_{asbs} + L_{ascs}) \tag{48}$$

$$L_{13}^{ss} = \frac{2}{3}(L_{asas} - .5L_{bsbs} - .5L_{cscs} + .5L_{asbs} + .5L_{ascs} - L_{bscs}) \tag{49}$$

$$L_{21}^{ss} = \frac{1}{\sqrt{3}}(.5L_{bsbs} - .5L_{cscs} - L_{asbs} + L_{ascs}) \tag{50}$$

$$L_{22}^{ss} = \frac{1}{2}(L_{bsbs} + L_{cscs} - 2L_{bscs}) \tag{51}$$

$$L_{23}^{ss} = \frac{1}{\sqrt{3}}(-L_{bsbs} + L_{cscs} - L_{asbs} + L_{ascs}) \tag{52}$$

$$L_{33}^{ss} = \frac{1}{3}(L_{asas} + L_{bsbs} + L_{cscs} + 2L_{asbs} + 2L_{ascs} + 2L_{bscs}) \tag{53}$$

and $L_{31}^{ss} = \frac{1}{2}L_{13}^{ss}$, and $L_{32}^{ss} = \frac{1}{2}L_{23}^{ss}$. When $N_a = N_b = N_c$, $N_{asas} = N_{bsbs} = N_{cscs}$ and $N_{asbs} = N_{ascs} = N_{bscs}$. By using Eqs. (7)–(13) it can be shown that $L_{12}^{ss} = L_{13}^{ss} = L_{21}^{ss} = L_{23}^{ss} = L_{31}^{ss} = L_{32}^{ss} = 0$ and $L_{11}^{ss} = L_{22}^{ss} = L_{ls} + L_m$, $L_{33}^{ss} = L_{ls}$.

A.3. The stator-to-rotor qd0 mutual inductances

Because of rotor symmetry, the coefficients of stator-to-rotor mutual inductances can be simplified as $N_{asar} = N_{asbr} = N_{ascr} = N_{asr}$, $N_{bsar} = N_{bsbr} = N_{bscr} = N_{bsr}$, and $N_{csar} = N_{csbr} = N_{cscr} = N_{csr}$, and the transformation result is

$$L_{11}^{sr} = L_{asr} + .25L_{bsr} + .25L_{csr} \tag{54}$$

$$L_{12}^{sr} = \frac{\sqrt{3}}{4}(L_{bsr} - L_{csr}) \tag{55}$$

$$L_{22}^{sr} = \frac{3}{4}(L_{bsr} + L_{csr}) \tag{56}$$

$$L_{31}^{sr} = .5L_{asr} - .25L_{bsr} - .25L_{csr} \tag{57}$$

$L_{21}^{sr} = L_{12}^{sr}$, and $L_{32}^{sr} = -L_{12}^{sr}$. When $N_a = N_b = N_c = N_s$, $L_{asar} = L_{asbr} = L_{ascr} = L_{bsar} = L_{bsbr} = L_{bscr} = L_{csar} = L_{csbr} = L_{cscr}$ and mutual inductances will be $L_{11}^{sr} = L_{22}^{sr} = \frac{N_r}{N_s}L_m$ and $L_{12}^{sr} = L_{21}^{sr} = L_{31}^{sr} = L_{32}^{sr} = 0$.

A.4. The rotor qd0 self- and mutual inductances

The rotor self- and mutual inductances are

$$L_{11}^{rr} = L_{22}^{rr} = L_{lr} + \frac{3}{2}L_{mar} = L_{lr} + \frac{N_r^2}{N_s^2}L_m \tag{58}$$

$$L_{33}^{rr} = L_{lr} \tag{59}$$

A.5. Matrix elements for induction motor with inter-turn stator short circuit

The stator *qd* self- and mutual inductances:

From (49) and (53), the stator *qd* self- and mutual inductances can be defined as follows

$$\begin{aligned} L_{11}^{ss} &= \frac{2}{3}(L_{asas} + .5L_{bsbs} - 2L_{asbs} + .5L_{bscs}) \\ &= \frac{2}{3}\left[(L'_{asas} + .5(L_{bsbs} + L_{bscs}) - 2L'_{asbs}) + (L_{assh} - L_{shbs})\right] + \frac{2}{3}\left[L_{shsh} + (L_{assh} - L_{shbs})\right] \\ &= (L_q^s + L_q^{ssh}) + (L_q^{sh} + L_q^{ssh}) \end{aligned} \tag{60}$$

$$\begin{aligned} L_{22}^{ss} &= \frac{1}{2}(L_{bsbs} + L_{cscs} - 2L_{bscs}) = L_{bsbs} - L_{bscs} \\ &= L_{ls} + L_m = L_d^s \end{aligned} \tag{61}$$

The stator-to-rotor *qd* mutual inductances:

From (54) and (55), the stator-to-rotor *qd* mutual inductances can be defined as follows:

$$\begin{aligned} L_{11}^{sr} &= L_{asr} + .25L_{bsr} + .25L_{csr} = L_{asr} + .5L_{bsr} \\ &= (L'_{asr} + .5L_{bsr}) + L_{shar} = L_q^{sr} + L_q^{shr} \end{aligned} \tag{62}$$

$$L_{22}^{sr} = \frac{3}{4}(L_{bsr} + L_{csr}) = \frac{3}{2}L_{bsr} = L_d^{sr} \quad (63)$$

The rotor self- and mutual inductances and resistances will be the same as before.

A.6. Motor parameters

Reliance motor parameters:

Line voltage	460 V	Total number of turns per phase	252
Full load line current	2.7 A	Stator winding resistance	4.05 Ω
Horse power	2 hp	Stator leakage inductance	13.97 mH
Rated speed at 60 Hz	1752 rpm	Rotor resistance (stator referred)	2.6 Ω
Number of poles	4	Rotor leakage inductance (stator referred)	13.97 mH
Power factor	0.815	Magnetising inductance	538.68 mH
Service factor	1.15	Rotor inertia	0.06 kg m^2

References

[1] W.T. Thomson, A review of on-line condition monitoring techniques for three-phase squirrel-cage induction motors – past present and future, in: Proceedings of the 1999 IEEE International Symposium on Diagnostics for Electrical Machines, Power Electronics and Drives, IEEE SDEMPED'99, 1999, pp. 3–18.

[2] M. Arkan, Stator Fault Diagnosis in Induction Motors, University of Sussex, Ph.D. Thesis, 2000.

[3] R.M. Tallam, T.G. Habetler, R.G. Harley, Transient Model for Induction Machines with Stator Winding Turn Faults, in: Proceedings of the IEEE Industry Applications Conference 35th Annual Meeting-World Conference on Industrial Applications of Electrical Energy, Rome, Italy, October 2000, 2000.

[4] M. Arkan, D. Kostic-Perovic, P.J. Unsworth, Online stator fault diagnosis in induction motors, IEE Proceedings: Electric Power Applications 148 (6) (2001) 537–547.

[5] G.B. Kliman, W.J. Premerlani, R.A. Koegl, D. Hoeweler, A New Approach to On-Line Turn Fault Detection in AC Motors, in: IAS Annual Meeting, October 1996, 1996, pp. 687–693.

[6] J.E. Brown, O.I. Butler, A general method of analysis of three phase induction motors with asymmetrical primary connections, Proc. IEE 100 (1953) 25–34.

[7] C.S. Jha, S.S. Murthy, Generalised rotating-field theory of wound-rotor induction machines having asymmetry in stator and/or rotor windings, Proc. IEE 120 (8) (1973).

[8] X. Luo, Y. Liao, H.A. Toliyat, T.A. Lipo, Multiple coupled circuit modelling of induction machines, IEEE Trans. Ind. Appl. 31 (2) (1995) 311–317.

[9] H.A. Toliyat, T.A. Lipo, Transient analysis of cage induction machines under stator, rotor bar end ring faults, IEEE Trans. Energy Convers. 10 (2) (1995) 241–247.

[10] G.M. Joksimovic, J. Penman, The detection of inter-turn short circuits in the stator windings of operating motors, IEEE Trans. Ind. Electron. 47 (5) (2000) 1078–1084.

[11] S. Williamson, K. Mirzoian, Analysis of cage induction motors with stator winding faults, IEEE Trans. Power Apparatus Syst. PAS-104 (7) (1985) 1838–1842.

[12] A. Consoli, T.A. Lipo, Orthogonal axis models for asymmetrically connected induction machines, IEEE Trans. Power Apparatus Syst. PAS-101 (12) (1982) 4518–4526.

[13] A.K. Wallace, E.S. Ward, A. Wright, Sources of harmonic currents in slip-ring motors, Proc. IEE 121 (12) (1974).

[14] M.Y. Chow, Methodologies of Using Neural Network and Fuzzy Logic Technologies for Motor Incipient Fault Detection, World Scientific Publication, 1997, ISBN 981-023265-9.

[15] D.W. Novotny, T.A. Lipo, Vector Control and Dynamics of AC Drives, Clarendon Press, Oxford, 1996.

[16] P. Krause, O. Wasynczuk, S.D. Sudhoff, Analysis of Electric Machinery, IEEE Inc, 1995, ISBN 0-7803-1101-9.

[17] P. Vas, Vector Control of AC Machines, Oxford Science Publications, 1999.

[18] C.M. Ong, Dynamic Simulation of Electric Machinery, Prentice Hall PTR, 1998, ISBN 013-723785-5.

[19] S.P. Huang, Active Mains Supply Harmonic Filtering, University of Sussex, Ph.D. Thesis, 1997.

[20] M. Arkan, P.J. Unsworth, Stator fault diagnosis in induction motors using power decomposition, in: Phoenix, USA, October, Proceedings of the IEEE Industry Applications Conference 34th Annual Meeting, 1999, vol. 3, pp. 1908–1912.

[21] D. Kostic-Perovic, M. Arkan, P.J. Unsworth, Induction motor fault detection by space vector angular fluctuation, in: Proceedings of IEEE Industry Applications Conference 35th Annual Meeting-World Conference on Industrial Applications of Electrical Energy, Rome, Italy, October, 2000.